AMERICAN SOCIETY FOR MICROBIOLOGY | Journal of Virology

Human T-Lymphotropic Virus Type 1-Induced Overexpression of Activated Leukocyte Cell Adhesion Molecule (ALCAM) Facilitates Trafficking of Infected Lymphocytes through the Blood-Brain Barrier

Céline Curis,[a,b,c,d] Florent Percher,[a,b,c] Patricia Jeannin,[a,b] Thomas Montange,[a,b] Sébastien A. Chevalier,[e] Danielle Seilhean,[f] Luis Cartier,[g] Pierre-Olivier Couraud,[h] Olivier Gout,[i] Antoine Gessain,[a,b] Pierre-Emmanuel Ceccaldi,[a,b,c] Philippe V. Afonso[a,b]

Unité d'Epidémiologie et Physiopathologie des Virus Oncogènes, Département de Virologie, Institut Pasteur, Paris, France[a]; Centre National de la Recherche Scientifique (CNRS) UMR 3569, Paris, France[b]; Cellule Pasteur, Université Paris Diderot, Sorbonne Paris Cité, Paris, France[c]; Master Biosciences, Ecole Normale Supérieure (ENS) de Lyon, Lyon, France[d]; Equipe Oncogenèse Rétrovirale, ENS de Lyon, and Equipe labélisée Ligue Nationale Contre le Cancer, Centre International de Recherche en Infectiologie, INSERM U1111, CNRS UMR 5308, Lyon, France[e]; Département de Neuropathologie, Groupe Hospitalier Pitié-Salpêtrière, Assistance Publique-Hôpitaux de Paris, Université Pierre et Marie Curie, Sorbonne Universités, Paris, France[f]; Departamento de Ciencias Neurológicas, Facultad de Medicina, Universidad de Chile, Santiago, Chile[g]; Institut Cochin, INSERM U1016, CNRS UMR 8104, Université Paris Descartes, Sorbonne Paris Cité, Paris, France[h]; Service de Neurologie, Fondation Ophtalmologique Adolphe de Rothschild, Paris, France[i]

ABSTRACT

Human T-lymphotropic virus type 1 (HTLV-1) is the etiological agent of a slowly progressive neurodegenerative disease, HTLV-1-associated myelopathy/tropical spastic paraparesis (HAM/TSP). This disease develops upon infiltration of HTLV-1-infected lymphocytes into the central nervous system, mostly the thoracic spinal cord. The central nervous system is normally protected by a physiological structure called the blood-brain barrier (BBB), which consists primarily of a continuous endothelium with tight junctions. In this study, we investigated the role of activated leukocyte cell adhesion molecule (ALCAM/CD166), a member of the immunoglobulin superfamily, in the crossing of the BBB by HTLV-1-infected lymphocytes. We demonstrated that ALCAM is overexpressed on the surface of HTLV-1-infected lymphocytes, both in chronically infected cell lines and in primary infected CD4$^+$ T lymphocytes. ALCAM overexpression results from the activation of the canonical NF-κB pathway by the viral transactivator Tax. In contrast, staining of spinal cord sections of HAM/TSP patients showed that ALCAM expression is not altered on the BBB endothelium in the context of HTLV-1 infection. ALCAM blockade or downregulation of ALCAM levels significantly reduced the migration of HTLV-1-infected lymphocytes across a monolayer of human BBB endothelial cells. This study suggests a potential role for ALCAM in HAM/TSP pathogenesis.

IMPORTANCE

Human T-lymphotropic virus type 1 (HTLV-1) is the etiological agent of a slowly progressive neurodegenerative disease, HTLV-1-associated myelopathy/tropical spastic paraparesis (HAM/TSP). This disease is the consequence of the infiltration of HTLV-1-infected lymphocytes into the central nervous system (CNS), mostly the thoracic spinal cord. The CNS is normally protected by a physiological structure called the blood-brain barrier (BBB), which consists primarily of a continuous endothelium with tight junctions. The mechanism of migration of lymphocytes into the CNS is unclear. Here, we show that the viral transactivator Tax increases activated leukocyte cell adhesion molecule (ALCAM/CD166) expression. This molecule facilitates the migration of lymphocytes across the BBB endothelium. Targeting this molecule could be of interest in preventing or reducing the development of HAM/TSP.

Human T-lymphotropic virus type 1 (HTLV-1) is a retrovirus discovered in 1980 (1). HTLV-1 is estimated to infect at least 10 million people worldwide, with a heterogeneous geographical distribution: the main foci of high endemicity are southern Japan, the Caribbean, South America, and equatorial Africa (2). Among HTLV-1-infected individuals, 90 to 95% remain asymptomatic throughout their lives. Nevertheless, HTLV-1 is the etiological agent of two severe diseases: adult T cell leukemia/lymphoma (ATLL), an aggressive T cell malignancy which affects around 5% of HTLV-1-infected individuals (3), and HTLV-1-associated myelopathy/tropical spastic paraparesis (HAM/TSP), a chronic inflammatory disease of the central nervous system (CNS) which develops in 0.2 to 3% of infected individuals (4).

HAM/TSP is clinically identified as a progressive motor and sensory disturbance of the lower limbs (5). HAM/TSP is typically characterized by the presence of the Babinski response and spasticity associated with limb weakness and autonomic dysfunction, slowly leading to paralysis. The pathophysiology of HAM/TSP is not fully understood (6). The main feature is perivascular lymphocyte infiltration in the thoracic region of the spinal cord, which is responsible for myelin and axonal degeneration and spi-

Received 22 March 2016 Accepted 25 May 2016

Accepted manuscript posted online 1 June 2016

Citation Curis C, Percher F, Jeannin P, Montange T, Chevalier SA, Seilhean D, Cartier L, Couraud P-O, Gout O, Gessain A, Ceccaldi P-E, Afonso PV. 2016. Human T-lymphotropic virus type 1-induced overexpression of activated leukocyte cell adhesion molecule (ALCAM) facilitates trafficking of infected lymphocytes through the blood-brain barrier. J Virol 90:7303–7312. doi:10.1128/JVI.00539-16.

Editor: S. R. Ross, University of Illinois at Chicago College of Medicine

Address correspondence to Philippe V. Afonso, pafonso@pasteur.fr.

C.C. and F.P. contributed equally to this article.

nal cord atrophy observable by magnetic resonance imaging (MRI) (7). Clonal populations of HTLV-1-infected lymphocytes are found in the cerebrospinal fluid and are derived from the same HTLV-1-infected progenitors as peripheral blood infected lymphocytes (8). This demonstrates that HTLV-1-infected lymphocytes can migrate between the blood and the CNS compartments in HAM/TSP.

Normally, the CNS is protected from infectious agents by a selective barrier: the blood-brain barrier (BBB). The BBB is a dynamic physiological interface between the blood and the CNS. It is composed of three cell types: brain microvascular endothelial cells, astrocytes (through their endfeet), and pericytes (9). Tight junctions seal the endothelial cells together to form a selective barrier responsible for maintaining CNS fluid homeostasis and protecting neural tissues from toxins and infectious agents (10). The tight junctions of the BBB endothelium in HAM/TSP patients are locally disorganized; this allows T cells to transmigrate into the CNS, resulting in neuroinflammation (11, 12).

We investigated the potential role of the activated leukocyte cell adhesion molecule (ALCAM/CD166) in diapedesis to further understand the mechanisms of HTLV-1-infected lymphocyte transmigration through the BBB. ALCAM is a member of the immunoglobulin superfamily. There are two ALCAM ligands: ALCAM itself and CD6. ALCAM is expressed on endothelia and epithelia, where it participates in tissue development and maintenance (13); CD6 is not expressed on endothelia (14). ALCAM downregulation on primary human umbilical vein endothelial cells reduces monocyte transmigration (15). Conversely, ALCAM overexpression on endothelia or epithelia usually enhances cell extravasation and metastasis (14, 16). ALCAM is also upregulated on the BBB endothelium in multiple sclerosis, thus promoting leukocyte trafficking into the CNS (17). Leukocytes express both ALCAM and CD6, which can interact with endothelial ALCAM. ALCAM has been implicated in monocyte interaction with the BBB and monocyte migration into the CNS during human immunodeficiency virus type 1 (HIV-1) infection (18–20).

We studied the role of ALCAM in HTLV-1 infection and HAM/TSP pathogenesis. We found that ALCAM is overexpressed on HTLV-1-infected T lymphocytes as a consequence of Tax-induced NF-κB activation. In contrast, *ex vivo* studies showed that ALCAM expression is not altered on the BBB endothelium during HAM/TSP. Finally, ALCAM blockade or downregulation of ALCAM reduced transmigration of HTLV-1-infected lymphocytes in an *in vitro* BBB model.

MATERIALS AND METHODS

Cells and tissues. T cells chronically infected with HTLV-1 (HUT-102, C91/PL, and C81-66) and control (CEM and Jurkat) T cells were grown in RPMI medium (Gibco, Life Technologies) supplemented with 10% fetal bovine serum (FBS) and 1% penicillin-streptomycin (PS). Bay 11-7082 (Abcam) was added to the culture medium for 24 h, where indicated below. Of note, cell viability was not affected by Bay 11-7082 treatment. The human cerebral microvascular endothelial cell line hCMEC/D3 was provided by P.-O. Couraud (21) and grown on collagen I/fibronectin-coated plates in EBM-2 (Lonza) supplemented with 5% FBS, 1% PS, 1% chemically defined lipid concentrate (Invitrogen), 10 mM HEPES (Sigma-Aldrich), 1.4 μM hydrocortisone (Sigma-Aldrich), 1.5 $\mu g \cdot ml^{-1}$ of ascorbic acid (Sigma-Aldrich), and 200 $ng \cdot ml^{-1}$ of basal fibroblast growth factor (Sigma-Aldrich). 293T cells were grown in Dulbecco modified Eagle medium (DMEM; Gibco) supplemented with 10% FBS and 1% PS.

For the transduction of primary cells, the blood samples were provided by the EFS (Etablissement français du sang). Peripheral blood mononuclear cells (PBMCs) were obtained by Ficoll centrifugation and $CD4^+$ T lymphocytes were isolated by positive selection with magnetic beads (Miltenyi Biotech). Purity was higher than 95%. $CD4^+$ T cells were grown in RPMI medium with 10% FBS, 1% PS, and interleukin 2 (IL-2; 50 U/ml) and activated by phytohemagglutinin (PHA; 1 $\mu g \cdot ml^{-1}$) for 3 days.

We obtained PBMCs from healthy donors (HDs), HTLV-1 asymptomatic donors, and HAM/TSP patients in the context of a Biomedical Research Program approved by the Committee for the Protection of Persons, Ile-de-France II, Paris (2012-10-04 SC). All individuals gave informed consent.

Paraffin-embedded spinal cord sections correspond to the previously described anatomopathological specimen, obtained during postmortem examination (22, 23).

Flow cytometry analysis. Frozen PBMCs were thawed and cultured overnight in DMEM supplemented with 10% human serum. The cells were stained for viability (LIVE/DEAD; Life Technologies), ALCAM (clone 3A6; eBioscience), CD3 (clone UCHT1; Coulter), CD4 (clone RPA-T4; eBioscience), CD6 (clone M-T605; BD Pharmingen), or CD25 (clone BC96; eBioscience). Paraformaldehyde (PFA)-fixed samples were analyzed on an LSRII analyzer (BD Biosciences).

For cell lines, the cells were fixed with paraformaldehyde (2%) after ALCAM staining. All data were acquired using a FACScalibur (Becton Dickinson) and analyzed using FlowJo software (v10.0.8; FlowJo LCC). At least 10^5 events corresponding to viable cells were acquired.

For neoinfection, HUT-102 donor lymphocytes were irradiated (10 Gy), washed, and cultured with Jurkat cells at a 1:1 ratio. After 1 week, the cells were stained for ALCAM, fixed, permeabilized with a 0.1% Triton solution, stained with an anti-p24 primary antibody (clone 46/3.24.4, Abcam), revealed with the secondary antibody (Alexa Fluor 488; Life Technologies), and then analyzed by fluorescence-activated cell sorting (FACS).

Lentiviral vector production and transduction. Lentiviral vectors encoding Tax and/or green fluorescent protein (GFP) were described previously (24). HEK293T cells were transfected with psPAX-2 (encoding HIV Gag/Pol, 4.68 μg; Addgene), pMD2.G (vesicular stomatitis virus G protein [VSV-G], 2.52 μg; Addgene) and pSD101-FLAG-Tax (wild type [WT] or mutant)-internal ribosome entry site [IRES]-GFP (9 μg) plasmids. For short hairpin RNAs (shRNAs), the cells were transfected with psPAX-2, pMD2.G, and pGIPZ plasmids (9 μg) encoding *alcam* shRNA or nontargeting shRNA (CTRL sh) (GE Dharmacon). After 72 h, supernatants were collected, centrifuged, filtered at 0.45 μm, and stored at −80°C.

For Tax transduction, cell surface expression of ALCAM was assessed 72 h posttransduction for Jurkat cells and 96 h posttransduction for primary $CD4^+$ T cells. For shRNA transduction, the cells were selected for 10 days with puromycin (1 $\mu g \cdot ml^{-1}$) prior to migration assays.

Western blot analysis. Cell extracts were prepared from 10^6 cells lysed in radioimmunoprecipitation assay (RIPA) buffer containing protease inhibitors (Roche) for 30 min at 4°C. The protein concentration was determined using the Pierce bicinchoninic acid (BCA) protein assay (Life Technologies). The proteins were denatured for 15 min at 70°C, separated by electrophoresis on NuPAGE Novex 4 to 12% bis-Tris protein gels (Life Technologies), and transferred to a 0.2-μm nitrocellulose membrane using the Trans-Blot Turbo transfer system (Bio-Rad). The membrane was saturated with Tris-buffered saline with Tween 20 (TBST) plus 5% bovine serum albumin (BSA), incubated overnight at 4°C with the primary antibody (anti-Tax [Tab172; NIH], anti-GFP [clone JL-8; Clontech], or anti-β-tubulin [polyclonal; Santa Cruz]), washed three times with TBST, incubated for 1 h with the secondary antibody, and washed. The results were obtained using the Odyssey CLx infrared imaging system (LI-COR Biosciences).

TABLE 1 Primer list for promoter analysis

Primer pair	Primer sequence[a]
−400 prALCAM	F: 5′-ATATATGAGCTCCAGAAAGTGTTAGTCCCAGG-3′ R: 5′-AGAGAAAGCTTGGTGCTAAGAAGGACTCG-3′
−1000 prALCAM	F: 5′-ATATATGAGCTCAAATCACCGCTTAACTCAAAG-3′ R: 5′-AGAGAAAGCTTGGTGCTAAGAAGGACTCG-3′
prALCAM Δ site 1	F: 5′-CTTTTGTAGACATTGTATGACGAAGTACGG-3′ R: 5′-CCGTACTTCGTCATACAATGTCTACAAAAG-3′
prALCAM Δ site 2	F: 5′-GAATCAGTCCAGTGCCAACAAGTAG-3′ R: 5′-CTACTTGTTGGCACTGGACTGATTC-3′

[a] F, forward; R, reverse.

Reverse transcription (RT)-qPCR. Total cellular RNA was extracted using the RNeasy Plus minikit (Qiagen). cDNA was synthesized from 500 ng of RNA using Superscript II reverse transcriptase (Invitrogen). The *alcam* mRNA level was quantified by SYBR green-based quantitative PCR (qPCR) using an Eppendorf realplex^2 thermal cycler (15 min at 95°C and then 40 cycles of 15 s at 95°C, 20 s at 60°C, and 30 s at 72°C). *GAPDH* was used as a housekeeping gene. qPCR efficiency was determined by serial dilution of the samples (25). The primers were as follows: for human ALCAM (hALCAM), 5′-TCCTGCCGTCTGCTCTTCT-3′ (forward) and 5′-TTCTGAGGTACGTCAAGTCGG-3′ (reverse), and for human glyceraldehyde-3-phosphate dehydrogenase (hGAPDH), 5′-GGAGCGAGATCCCTCCAAAAT-3′ (forward) and 5′-GGCTGTTGTCATACTTCTCATGG-3′ (reverse).

ChIP assay. Chromatin immunoprecipitation (ChIP) assays were performed using the Pierce Agarose ChIP kit (Thermo Scientific). C81-66 cells were cross-linked and lysed, and the DNA was sheared by micrococcal nuclease digestion to obtain <900-bp DNA fragments. The chromatin extracts were incubated overnight at 4°C with 10 μg of antibodies (polyclonal rabbit IgG, anti-PolII, anti-p52, anti-p65 [Abcam], and anti-Tax [Tab 172; NIH]). The immune complexes were collected the next day by the addition of magnetic protein A beads (Thermo Scientific) and washed, stepwise, according to the manufacturer's protocol. Cross-linking was reversed by proteinase K digestion, and the resulting DNA was purified. qPCR, amplifying kB site 1, was performed using the following primers: 5′-AATCACCGCTTAACTAAAG-3′ (forward) and 5′-TATTTGCTTTTCCCGGG-3′ (reverse). The PCR products were visualized on a 3% agarose gel.

Immunohistofluorescence. Spinal cord sections (5 μm thick) were deparaffinized and fixed in acetone. Staining with the primary antibodies was performed after saturation with 10% normal donkey serum. The following primary antibodies were used: anti-ALCAM (polyclonal goat antibody; R&D) and anti-factor VIII (polyclonal rabbit antibody; Dako). Specific secondary antibodies were coupled with either Alexa Fluor 488 (Life Technologies) or Dylight 549 (Pierce). The sections were mounted in DAPI Fluoromount-G (Southern Biotech) and observed with an ApoTome.2 microscope (Zeiss). Quantification of the signal intensity was performed on 5 linear sections per image using Fiji software as previously described (17).

Cellular transmigration assay. Lymphocyte transmigration through an hCMEC/D3 monolayer cultured on a 3-μm-porosity Transwell filter (Corning) was determined by adding 2×10^5 lymphocytes to the upper compartment and counting the cells present in the lower compartment after 24 h. Where indicated, lymphocytes migrated in the presence of antibodies (30 $\mu g \cdot ml^{-1}$; anti-human ALCAM blocking antibody, anti-human CD6 blocking antibody, or mouse IgG1 isotype control; R&D Systems). We confirmed that the antibodies have no effect on endothelial integrity under the conditions used; i.e., they do not alter monolayer permeability.

For the migration assay with primary cells, $CD4^+$ T cells were isolated from PBMCs by negative selection using magnetic beads (Miltenyi Biotech), and 5×10^5 T cells were added onto the hCMEC/D3 cells.

Luciferase reporter assay. *alcam* promoter fragments (truncated at bp −1000 or −400) were amplified by PCR (Table 1) and cloned into a pGL2 basic luciferase vector (Promega). Site-directed mutagenesis was performed on the pGL2 bp −1000 *alcam* reporter plasmid using the QuikChange II XL site-directed mutagenesis kit (Agilent Technologies) and primers in Table 1.

293T cells (6×10^5) were transfected with 300 ng of pGL2-*alcam* promoter plasmids and 100 ng of empty pSG5M or pSG5M-Tax plasmid using LipoD293 (SignaGen) according to the manufacturer's instructions. Luciferase activity was measured 24 h after transfection with the luciferase assay system (Promega), and chemiluminescence was detected using an EnSpire multimode plate reader (PerkinElmer). The protein concentration was determined using the DC protein assay (Bio-Rad) to normalize for luciferase activity.

Statistical analyses. Analyses were performed using Prism software (v.6; GraphPad). Results were considered to be significant when the *P* value was <0.05.

RESULTS

HTLV-1-infected lymphocytes have high levels of ALCAM on their cell surface. We analyzed the cell surface levels of both ALCAM and CD6 on primary HTLV-1-infected $CD4^+$ T cells. PBMCs collected from noninfected healthy donors (HDs), asymptomatic HTLV-1 carriers (HACs), and HAM/TSP patients ($n = 6$ for each group) were immunostained for CD3, CD4, CD25, ALCAM, and CD6 and analyzed by flow cytometry.

The $CD3^+$ $CD4^+$ population was divided into 3 subpopulations based on CD25 levels. According to the literature, $CD25^-$ cells correspond to nonactivated lymphocytes and $CD25^+$ cells correspond to activated T cells (26). The $CD25^{++}$ population is composed of both T regulatory lymphocytes (Tregs) and HTLV-1-infected cells (27–29). Thus, the size of the $CD25^{++}$ population was larger for infected individuals (both HACs or HAM/TSP patients) than for HDs (Fig. 1A), and the percentage of $CD4^+$ $CD25^{++}$ cells correlates with proviral load (Fig. 1B).

The levels of CD6 were identical for all $CD4^+$ T cell subpopulations and were unaffected by the clinical status of the individuals (Fig. 1C). In contrast, the Treg population ($CD3^+$ $CD4^+$ $CD25^{++}$) of HDs had significantly higher levels of ALCAM than nonactivated or activated $CD4^+$ T cells ($P < 10^{-4}$, Friedman test, Dunn's *post hoc* test) (Fig. 1D). The level of ALCAM on the $CD25^{++}$ subpopulation of cells from infected individuals (i.e., mostly HTLV-1-infected cells) was high and similar to that of

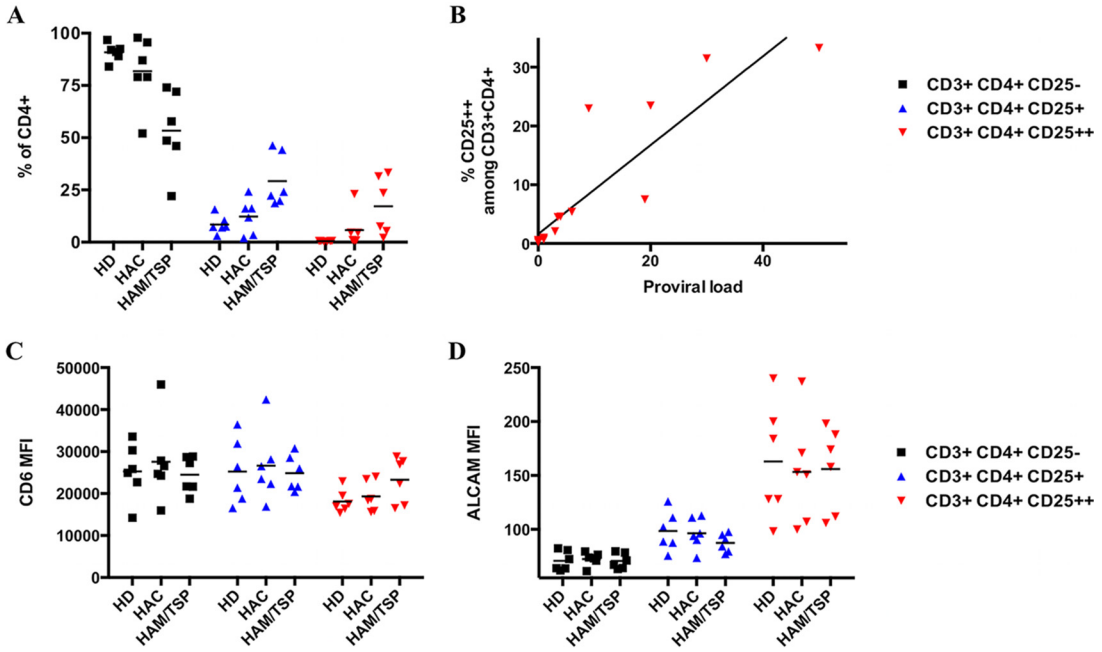

FIG 1 ALCAM is overexpressed on primary HTLV-1-infected $CD4^+$ T lymphocytes. (A) Percentage of the primary $CD4^+$ T lymphocyte subsets based upon CD25 levels by flow cytometry. Subpopulations correspond to nonactivated $CD4^+$ T cells ($CD25^-$, in black) or activated $CD4^+$ T cells ($CD25^+$, in blue). The $CD25^{++}$ subpopulation (in red) corresponds to Tregs in healthy donors (HDs) and mostly HTLV-1-infected cells in HTLV-1-infected asymptomatic carriers (HACs) and HAM/TSP patients. (B) The percentage of $CD4^+$ $CD25^{++}$ cells correlates with proviral load. Proviral load was calculated as a number of copies of Tax for 100 $CD4^+$ T cells. Spearman's correlation test was significant ($P < 10^{-4}$; Spearman's correlation coefficient [r_s] = 0.9796). (C) Mean fluorescence intensity (MFI) of CD6 on the different CD25-based subpopulations. (D) ALCAM MFI on the different CD25-based subpopulations.

Tregs (Fig. 1D). Thus, HTLV-1-infected cells express high levels of ALCAM.

Similarly, ALCAM levels were systematically higher on T cells chronically infected with HTLV-1 (e.g., HUT-102, C91/PL, and C81-66) than uninfected control cell lines (e.g., Jurkat and CEM) (Fig. 2A). To see whether the increase in ALCAM levels is a direct consequence of HTLV-1 infection, we infected Jurkat cells through coculture with irradiated HUT-102 cells, as previously described (30). The newly infected Jurkat cells (as assessed by expression of the viral p24 protein) had significantly higher levels of ALCAM on their surface than the uninfected cells present in the same culture (Fig. 2B).

Together, these data demonstrate that cell surface ALCAM increases upon HTLV-1 infection of $CD4^+$ T lymphocytes (both chronically infected cell lines and primary cells).

ALCAM overexpression is dependent on NF-κB activation by the viral transactivator Tax. We hypothesized that the viral transactivator Tax is the causative agent of HTLV-1-mediated ALCAM overexpression. We transduced Jurkat cells with lentiviral vectors encoding Tax together with GFP as a reporter (Tax IRES GFP vector) or GFP alone under conditions where the transduction efficiency was 50%; cell survival was more than 90% under these conditions. Tax was detected by Western blotting 72 h posttransduction (Fig. 2D). The level of ALCAM was higher on Tax-expressing cells than on control cells expressing GFP alone (Fig. 2C and E). Tax-induced ALCAM overexpression was also confirmed on primary $CD4^+$ T cells (Fig. 2F).

We tested whether ALCAM overexpression was associated with an increase in *alcam* mRNA levels, as Tax is a transactivator. We found that *alcam* levels were higher in T cell lines chronically infected with HTLV-1(HUT-102, C91/PL, and C81-66) than in control cell lines (Jurkat and CEM) (Fig. 3A). We observed a 5-fold increase in *alcam* levels in Tax-expressing Jurkat cells compared to GFP-expressing cells following transduction with the lentiviral vectors (Fig. 3B). Thus, Tax expression induces an increase in *alcam* transcription.

Tax is known to activate multiple cellular pathways, including the CREB and NF-κB pathways, involved in viral transcription and viral pathogenesis, respectively (31). We tested the capacity of 2 Tax-1 mutants to transactivate *alcam*. The Tax-1 M22 mutant activates the CREB pathway but is unable to activate the NF-κB pathway, and the Tax-1 M47 mutant is unable to activate the CREB pathway but activates the NF-κB pathway (32). We found that M22, but not M47, fails to activate *alcam* transcription (Fig. 3B), suggesting a central role of NF-κB in Tax-induced *alcam* transcription. To confirm the importance of this cellular pathway, we treated infected cells with the NF-κB pathway inhibitor Bay 11-7082 (33), which led to a dose-dependent decrease in *alcam* expression (Fig. 3C). Thus, activation of the NF-κB pathway is implicated in HTLV-associated *alcam* overexpression.

Previous studies have reported the presence of two potential κB sites in this region, located between −973 and −962 (κB 1), and −765 and −754 (κB 2) nucleotides upstream of the initiation codon, on the human *alcam* promoter (34, 35). We investigated which site on the *alcam* promoter participates in Tax-induced promoter activation. Using a luciferase assay, we found that Tax activates *alcam* transcription using a site between bp −1000 and bp −400 upstream of the initiation codon (Fig. 3D). By separately deleting the κB sites on the *alcam* promoter, we found that the distal κB site participated in Tax-induced promoter activation,

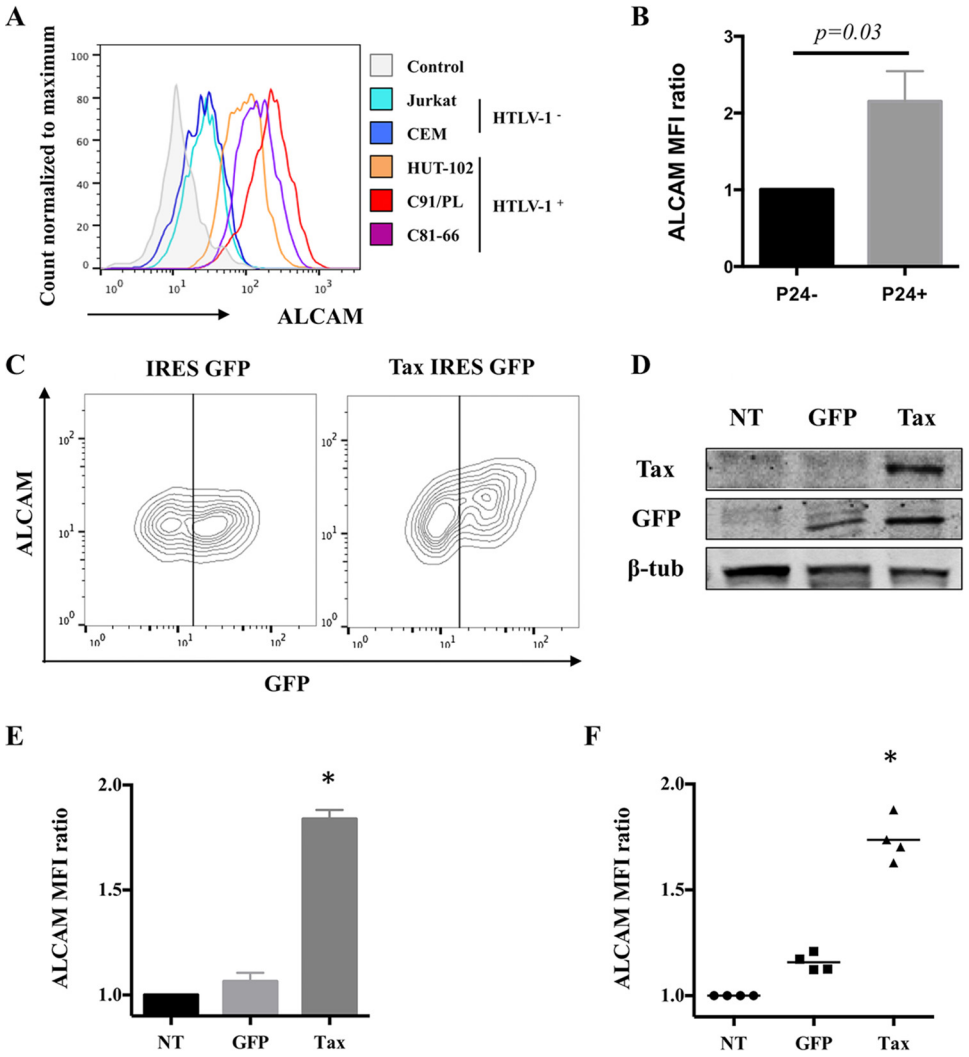

FIG 2 ALCAM levels are increased by Tax upon HTLV-1 infection. (A) ALCAM levels of the different cell lines. Cell surface ALCAM levels were measured by FACS on uninfected (Jurkat and CEM) or infected (HUT-102, C91/PL, and C81-66) lymphocytes. The control corresponds to isotype antibody staining. The graph is representative of the results of four independent experiments. (B) Newly infected cells overexpress ALCAM. Jurkat cells were cultured with 10-Gy-irradiated HUT-102 cells at a 1:1 ratio. After 1 week, p24 staining was monitored to assess for HTLV-1 neoinfection. The graph presents the ALCAM MFI means ± standard deviations (SD) for four independent experiments (normalized to Jurkat cells). The *P* value is calculated using the Wilcoxon test. (C to E) Tax-expressing Jurkat cells overexpress ALCAM. Jurkat cells were transduced with lentiviral vectors encoding GFP or Tax IRES GFP to achieve 50% transduction. (C) ALCAM and GFP were detected by FACS; the graph is representative of the results of four independent experiments. (D) Tax, GFP, and β-tubulin were detected in cellular extracts of nontransduced (NT) or GFP- or Tax-transduced Jurkat cells by Western blotting. (E) ALCAM MFI was normalized to NT cells (mean ± SD; $n = 4$). (E) ALCAM MFI was normalized to NT cells (mean ± SD; $n = 4$). *, significance ($P < 10^{-4}$, Friedman test, Dunn's *post hoc* test). (F) Tax-expressing primary $CD4^+$ T cells overexpress ALCAM. $CD4^+$ T cells were transduced with GFP or Tax-IRES-GFP lentiviral vectors and ALCAM levels were assessed by FACS. The results were normalized to NT cells (mean ± SD; $n = 4$ independent donors). *, significance ($P < 10^{-4}$, Friedman test, Dunn's *post hoc* test).

while deletion of the proximal one had no impact on *alcam* transcription (Fig. 3D).

Tax can activate both the canonical and noncanonical NF-κB pathways (36). We performed a chromatin immunoprecipitation assay (ChIP) and determined which proteins are present on the *alcam* promoter to determine which NF-κB pathway is associated with *alcam* overexpression. Both Tax and p65 were present on the *alcam* promoter, whereas p52 NF-κB was absent (Fig. 3E).

We have demonstrated that Tax increases *alcam* transcription, via the direct recruitment of the canonical NF-κB complex to the −973/−962 κB site on its promoter, resulting in ALCAM overexpression at the cell surface of HTLV-1-infected lymphocytes.

ALCAM expression on the BBB endothelium remains unchanged during HAM/TSP. ALCAM, but not CD6, is overexpressed on HTLV-1-infected lymphocytes. We investigated whether ALCAM is also overexpressed on the BBB endothelium in the context of HTLV-1 infection, as shown for multiple sclerosis (17).

We compared ALCAM expression levels on thoracic spinal cord sections of uninfected individuals ($n = 3$) and HAM/TSP patients ($n = 2$). Immunoreactivity for factor VIII, an endothelial cell marker, was assessed to verify that the sections were well conserved and comparable. ALCAM immunoreactivity colocalized with factor VIII, showing that ALCAM is expressed on the BBB endothelium in the thoracic spinal cord. We did not observe any

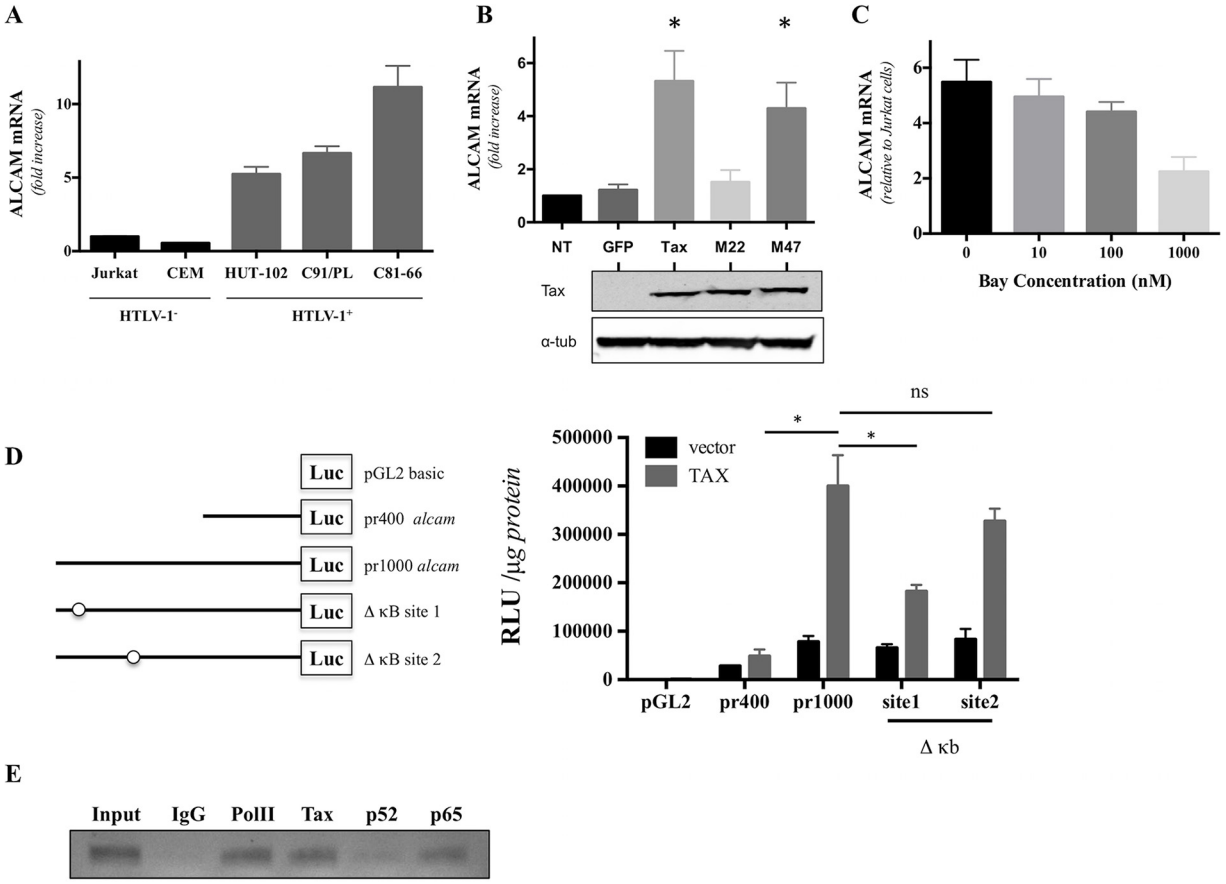

FIG 3 The canonical NF-κB pathway upregulates *alcam* expression via Tax transactivation. (A) *alcam* expression is higher in cells chronically infected with HTLV-1. *alcam* mRNA levels were assessed by RT-qPCR in uninfected (Jurkat and CEM) or infected (HUT-102, C91/PL, and C81-66) lymphocytes. The data were normalized to *GAPDH* expression and Jurkat cells. The graph presents means ± SDs from four independent experiments. (B) *alcam* is overexpressed in Jurkat cells upon transduction with Tax proteins competent for NF-κB activation. *alcam* mRNA levels were assessed by RT-qPCR on Jurkat cells transduced with lentiviral vectors encoding GFP or Tax (WT or mutants M22 and M47)-IRES-GFP. The data were normalized to *GAPDH* expression and nontransduced (NT) Jurkat cells. Theraph represents means ± SDs from four independent experiments. *, significance ($P < 10^{-4}$, Friedman test, Dunn's *post hoc* test). (C) NF-κB inhibition reduced *alcam* mRNA levels. Jurkat and C91/PL cells were cultured with different concentrations of Bay 11-7082. *alcam* mRNA levels were assessed by RT-qPCR after 24 h of treatment. The graph presents means ± SEMs of ALCAM mRNA from three independent experiments. (D) The κB site 1 (at position −962) is involved in Tax-mediated *alcam* transactivation. 293T cells were transfected with pGL2-basic vectors encoding luciferase under the control of the *alcam* promoter (either a 400-bp (pr400) or a 1,000-bp (pr1000) segment, or the pr1000 lacking a κB site: site 1 or site 2), together with the pSG5M or pSG5M-Tax plasmids. Luciferase activity (relative light units [RLU]) was normalized to the protein concentration. The graph presents the means ± SEMs from three independent experiments. *, significance ($P < 10^{-4}$, two-way ANOVA, Sidak's *post hoc* test). ns, not significant. (E) Tax directly recruits the canonical NF-κB complex to the *alcam* promoter. A ChIP assay was performed on C81-66 cells using IgG control, anti-RNA PolII (noted PolII, as a positive control), anti-Tax, anti-p52, and anti-p65 antibodies. A 140-bp DNA fragment corresponding to the *alcam* promoter was revealed on an agarose gel. The results are representative of those from three experiments.

difference in ALCAM immunoreactivity between samples from control and HAM/TSP patients (Fig. 4A). We quantified the ALCAM signal intensity and confirmed the absence of ALCAM overexpression on the BBB endothelium in the thoracic spinal cord of HAM/TSP patients (Fig. 4B).

In agreement with the spinal cord staining results, we showed, by immunofluorescence, that the ALCAM level and distribution pattern on a monolayer of human cerebral microvascular endothelial hCMEC/D3 cells were unaltered upon coculture with lymphocytes (infected or not with HTLV-1). Of note, similar to other endothelial cells (14), hCMEC/D3 cells do not express CD6.

We conclude that ALCAM expression is unaltered on BBB endothelial cells during HAM/TSP.

ALCAM is involved in the transmigration of lymphocytes chronically infected with HTLV-1 in an *in vitro* BBB model. We tested the impact of an anti-ALCAM blocking antibody (used in previous studies [17, 19, 20]) on the transmigration of T cell lines through a monolayer of human cerebral microvascular endothelial hCMEC/D3 cells cultured on a Transwell device to determine if ALCAM plays a role in the migration of HTLV-1-infected lymphocytes across the BBB. These cells have been extensively used as a relevant *in vitro* model for the human BBB endothelium (37). As CD6 is also expressed by HTLV-1-infected lymphocytes, we used an anti-CD6 blocking antibody to evaluate its potential role in migration as well.

Cells chronically infected with HTLV-1 migrated more than uninfected T cells in the presence of a control isotype antibody (Fig. 5A), in agreement with previous reports (12). Anti-CD6 blocking antibody had no significant impact on cell migration (infected or not) across the BBB model. The migration of uninfected cells was unaltered when anti-ALCAM blocking antibody was added, whereas the migration of HTLV-1 chronically infected

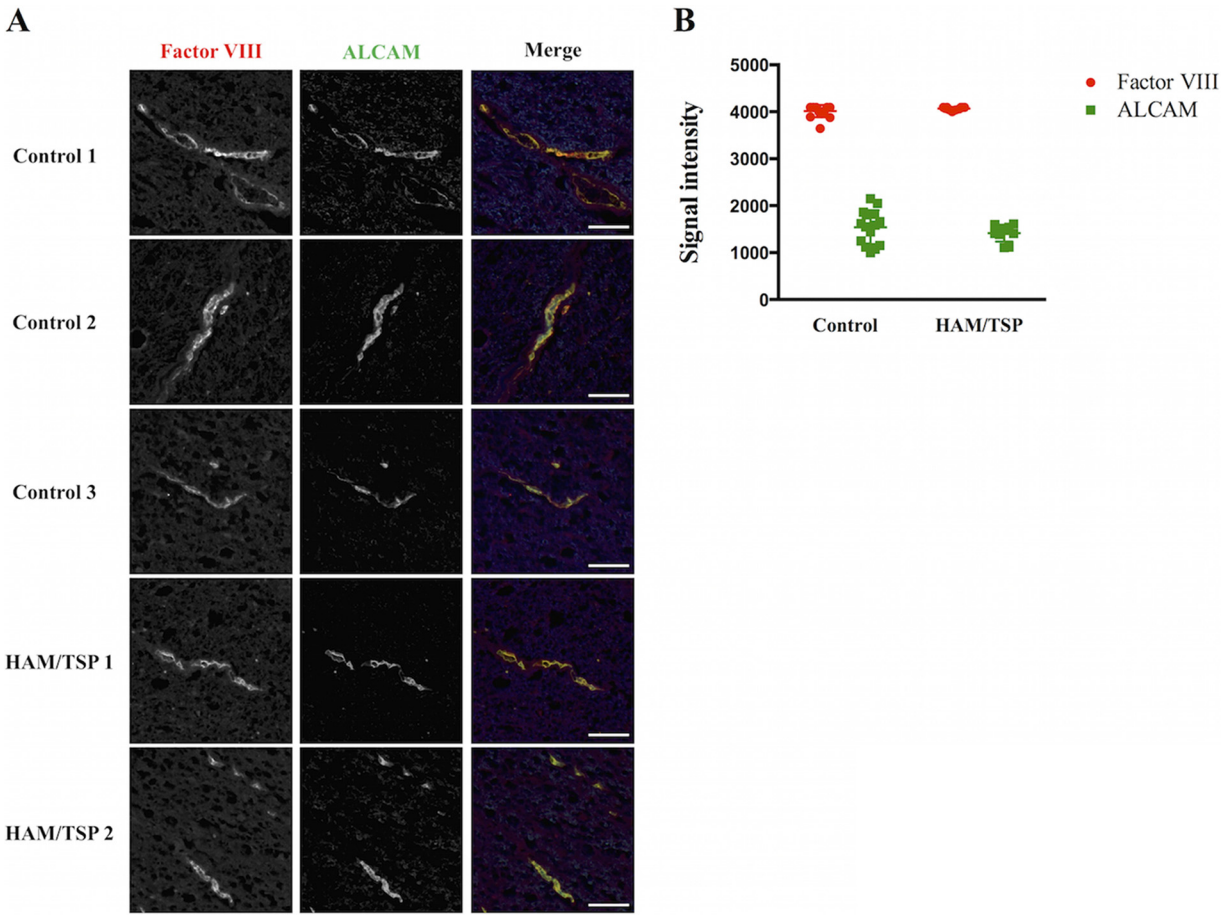

FIG 4 ALCAM expression on the thoracic spinal cord BBB endothelium is unchanged in HAM/TSP patients. (A) Spinal cord sections of control ($n = 3$) and HAM/TSP ($n = 2$) patients were immunostained for factor VIII (left) and ALCAM (right). In the merged image, factor VIII is presented in red, ALCAM in green, and nuclei in blue (4′,6-diamidino-2-phenylindole [DAPI] staining). Observations were performed using an ApoTome.2 microscope. The images are representative of the observed ALCAM and factor VIII immunoreactivities for each individual. Scale bar = 50 μm. (B) Quantification of ALCAM and factor VIII expressions on the BBB. Five distinct cross sections were defined for each vessel presented in panel A. Peak fluorescence signal intensity for each staining is reported. Horizontal line indicates the mean ± SD.

cells decreased significantly ($P < 10^{-4}$, two-way analysis of variance [ANOVA], Sidak *post hoc* test) (Fig. 5A). Thus, homotypic ALCAM interactions play a role in the transmigration of HTLV-1-infected cells in an *in vitro* BBB model.

We treated Jurkat and C91/PL cells with anti-*alcam* shRNAs to confirm that it is indeed the overexpression of ALCAM on lymphocytes that favors their transmigration (Fig. 5B). shRNA treatment had no impact on the ALCAM level on Jurkat cells, as the basal ALCAM level of these cells is already low. shRNA-expressing Jurkat cells migrated similarly to control cells (Fig. 5B). In contrast, shRNA treatment of C91/PL cells reduced the level of ALCAM and significantly reduced the capacity of these cells to migrate across the hCMEC/D3 monolayer ($P < 10^{-3}$ is considered significant; two-way ANOVA, Sidak *post hoc* test).

We isolated $CD4^+$ T cells from HDs or HAM/TSP patients and tested the impact of the anti-ALCAM antibody on the transmigration of these cells across an hCMEC/D3 monolayer (compared to the isotype antibody). We found that blocking ALCAM had no impact on the migration of $CD4^+$ T cells from HDs, whereas it significantly reduced the migration of the $CD4^+$ T cells from HAM/TSP patients (Fig. 5C).

In conclusion, ALCAM overexpression on HTLV-1 infected lymphocytes facilitates transmigration in an *in vitro* BBB model.

DISCUSSION

We showed that ALCAM is overexpressed on HTLV-1-infected lymphocytes (both cell lines and primary cells) and participates in their migration across an endothelial monolayer in a BBB model.

ALCAM levels increase in primary $CD4^+$ T cells upon HTLV-1 infection. The $CD3^+$ $CD4^+$ $CD25^{++}$ lymphocyte population corresponds to regulatory T cells (Tregs) in HD (27). A high level of ALCAM on Tregs was reported in a previous study (38). The $CD3^+$ $CD4^+$ $CD25^{++}$ subpopulation is enriched for HTLV-1-infected cells in infected donors (27, 28); indeed, upon HTLV-1 infection, CD25 is overexpressed (39). We found that HTLV-1-infected T cells have levels of ALCAM similar to those of Tregs. HTLV-1-infected cells exhibit a Treg-like phenotype based on their surface markers (e.g., CD25, CD45RO, and CD127) (40). Thus, ALCAM is another marker that is similarly expressed in these two populations.

We demonstrated that ALCAM overexpression on T cells can be mediated by the viral transregulator Tax at the transcriptional

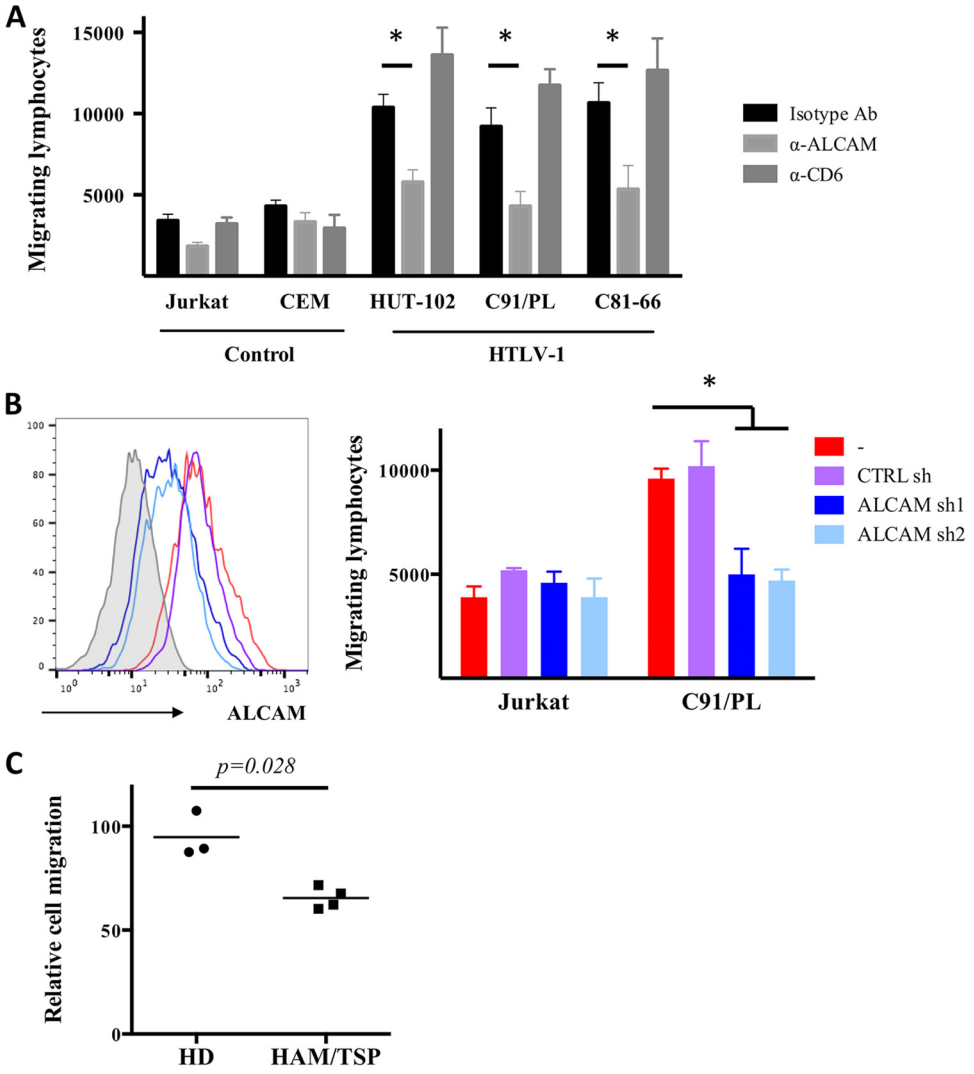

FIG 5 ALCAM is involved in the transmigration of HTLV-1-infected lymphocytes across a BBB endothelial monolayer. (A) Anti-ALCAM antibody reduces transmigration of HTLV-1-infected T cells through an hCMEC/D3 monolayer. Either uninfected T cells (Jurkat and CEM), or infected T cells (HUT-102, C91/PL, and C81-66) were added onto a monolayer of hCMEC/D3 cells, in the upper compartment of a Transwell device. Where indicated, anti-human ALCAM or anti-human CD6 blocking antibody or an IgG1 isotype control was added (30 $\mu g \cdot ml^{-1}$). Cell migration was determined after 24 h. The results represent the means ± SDs from three independent experiments. *, $P < 10^{-4}$ (considered significant), two-way ANOVA, Sidak *post hoc* test. (B) Downregulation of *alcam* reduces transmigration of HTLV-1-infected T cells through an hCMEC/D3 monolayer. Jurkat and C91/PL cells were transduced with lentiviral vectors encoding ALCAM shRNA (sh1 and sh2) or a nontargeting shRNA control. ALCAM expression was assessed by FACS (left side is a representative FACS for C91/PL cells), and transduced cells were then used for the migration assay (right side). The results represent the means ± SDs from three independent experiments. *, $P < 10^{-3}$ (significant), two-way ANOVA, Sidak *post hoc* test. (C) Anti-ALCAM antibody reduces transmigration of primary $CD4^+$ T cells from HAM/TSP patients through an hCMEC/D3 monolayer. $CD4^+$ T cells were isolated from PBMCs of HDs ($n = 3$) or HAM/TSP patients ($n = 4$) and added onto an hCMEC/D3 monolayer in the presence of antibodies (anti-ALCAM or isotype). The cells were allowed to migrate for 24 h. The data represent the percentages of cells that have migrated in the presence of the anti-ALCAM antibody relative to those that migrated in the presence of the isotype antibody. The *P* value was calculated using the Mann-Whitney test.

level, via the NF-κB pathway. *alcam* upregulation by Tax was previously suggested in microarray studies (24), although the role of the NF-κB pathway was not addressed. Tax directly recruits the canonical NF-κB complex to the promoter: it was previously shown that the p65 NF-κB subunit is able to bind to two functional κB sites, located −962 and −754 nucleotides upstream of the initiation codon, on the human *alcam* promoter (34, 35). We confirmed the functional role of the distal κB site here.

In some cases, ALCAM is overexpressed on endothelial cells and facilitates leukocyte transmigration. In pancreatic carcinoma, tumor-induced activation of the endothelium triggers the expression of ALCAM and facilitates Treg recruitment to the tumor (38). In multiple sclerosis, ALCAM expression increases on the BBB endothelium and facilitates pathogenic lymphocyte migration (17). In contrast, ALCAM was not found to be overexpressed in any part of the BBB endothelium of thoracic spinal cord sections of HAM/TSP patients. This is comparable to what has been reported for neurological disorders associated with HIV-1 infection (called neuroAIDS) (18). Nevertheless, BBB endothelial cells can be infected with HTLV-1 (11); thus, it is possible that HTLV-1-

infected endothelial cells could overexpress ALCAM and facilitate local extravasation. However, persistent infection of BBB endothelial cells appears to be a rare event (11).

We demonstrated that blockade or downregulation of ALCAM significantly reduced HTLV-1-infected lymphocyte migration through an endothelial monolayer in a BBB model. In contrast, blocking ALCAM did not significantly affect the migration of uninfected lymphocytes. A previous report has similarly shown that Th1 and Th17 migration through retinal vascular endothelium was ALCAM independent (41). Our data suggest that ALCAM plays a role in HAM/TSP pathogenesis similar to its role in neuroAIDS. Indeed, in neuroAIDS, ALCAM levels are not altered on the BBB endothelium (18), HIV infection increases ALCAM expression on monocytes (20), and ALCAM blockade by neutralizing antibodies reduces HIV-infected monocyte extravasation in *in vitro* BBB models (19, 20).

ALCAM expression facilitates migration of HTLV-1-infected lymphocytes across a BBB endothelial monolayer. Lymphocyte extravasation is a multistep process that involves rolling, adhesion, and transmigration (42). ALCAM does not directly participate in leukocyte adhesion to endothelium in a model consisting of THP-1 monocytes interacting with human umbilical vein endothelial cells (HUVECs) (15). However, ALCAM regulates actin dynamics during the lymphocyte-endothelium cross talk (43, 44). ALCAM is likely involved in the extravasation process, during transmigration.

ALCAM overexpression is not sufficient for efficient lymphocyte extravasation, although it facilitates the process. If ALCAM overexpression were sufficient, Treg infiltration into the CNS would be a frequent event. HTLV-1-infected lymphocytes migrate efficiently through the BBB because HTLV-1 infection modulates molecules that intervene in each step of the extravasation process. For example, HTLV-1-infected lymphocytes disrupt the tight junctions between endothelial cells through the secretion of inflammatory cytokines (12). Moreover, HTLV-1-infected lymphocytes adhere tightly to the endothelial cells (45). Endothelial ICAM-1 is essential for mediating shear-resistant arrest of $CD4^+$ effector T cells to the inflamed BBB endothelium (46), and p12-induced LFA1 clustering may participate in HTLV-1-infected T cell arrest (47).

In conclusion, ALCAM may be important for the onset of neuroinflammation and subsequent HAM/TSP pathogenesis. Targeting ALCAM may be useful for future therapeutic approaches.

ACKNOWLEDGMENTS

This work was supported by Ville de Paris Emergences Program. F.P. was funded by Région Ile de France through the DIM MALINF program. C.C. was funded by ENS de Lyon and Ministère de l'Enseignement Supérieur et de la Recherche.

We declare that no competing interests exist.

FUNDING INFORMATION

This work, including the efforts of Philippe V Afonso, was funded by Ville de Paris (Emergence). This work, including the efforts of Florent Percher, was funded by Region Ile de France (DIM MALINF). This work, including the efforts of Celine Curis, was funded by Ministère de l'Education Nationale (Ministry of Education, France).

REFERENCES

1. **Poiesz BJ, Ruscetti FW, Gazdar AF, Bunn PA, Minna JD, Gallo RC.** 1980. Detection and isolation of type C retrovirus particles from fresh and cultured lymphocytes of a patient with cutaneous T-cell lymphoma. Proc Natl Acad Sci U S A **77:**7415–7419. http://dx.doi.org/10.1073/pnas.77.12.7415.
2. **Gessain A, Cassar O.** 2012. Epidemiological aspects and world distribution of HTLV-1 infection. Front Microbiol **3:**388.
3. **Hinuma Y, Nagata K, Hanaoka M, Nakai M, Matsumoto T, Kinoshita KI, Shirakawa S, Miyoshi I.** 1981. Adult T-cell leukemia: antigen in an ATL cell line and detection of antibodies to the antigen in human sera. Proc Natl Acad Sci U S A **78:**6476–6480. http://dx.doi.org/10.1073/pnas.78.10.6476.
4. **Gessain A, Barin F, Vernant JC, Gout O, Maurs L, Calender A, de The G.** 1985. Antibodies to human T-lymphotropic virus type-I in patients with tropical spastic paraparesis. Lancet **ii:**407–410.
5. **Araujo AQ, Silva MT.** 2006. The HTLV-1 neurological complex. Lancet Neurol **5:**1068–1076. http://dx.doi.org/10.1016/S1474-4422(06)70628-7.
6. **Fuzii HT, da Silva Dias GA, de Barros RJ, Falcao LF, Quaresma JA.** 2014. Immunopathogenesis of HTLV-1-associated myelopathy/tropical spastic paraparesis (HAM/TSP). Life Sci **104:**9–14. http://dx.doi.org/10.1016/j.lfs.2014.03.025.
7. **Yamano Y, Sato T.** 2012. Clinical pathophysiology of human T-lymphotropic virus-type 1-associated myelopathy/tropical spastic paraparesis. Front Microbiol **3:**389.
8. **Cavrois M, Gessain A, Gout O, Wain-Hobson S, Wattel E.** 2000. Common human T cell leukemia virus type 1 (HTLV-1) integration sites in cerebrospinal fluid and blood lymphocytes of patients with HTLV-1-associated myelopathy/tropical spastic paraparesis indicate that HTLV-1 crosses the blood-brain barrier via clonal HTLV-1-infected cells. J Infect Dis **182:**1044–1050. http://dx.doi.org/10.1086/315844.
9. **Engelhardt B, Liebner S.** 2014. Novel insights into the development and maintenance of the blood-brain barrier. Cell Tissue Res **355:**687–699. http://dx.doi.org/10.1007/s00441-014-1811-2.
10. **Miller F, Afonso PV, Gessain A, Ceccaldi PE.** 2012. Blood-brain barrier and retroviral infections. Virulence **3:**222–229. http://dx.doi.org/10.4161/viru.19697.
11. **Afonso PV, Ozden S, Cumont MC, Seilhean D, Cartier L, Rezaie P, Mason S, Lambert S, Huerre M, Gessain A, Couraud PO, Pique C, Ceccaldi PE, Romero IA.** 2008. Alteration of blood-brain barrier integrity by retroviral infection. PLoS Pathog **4:**e1000205. http://dx.doi.org/10.1371/journal.ppat.1000205.
12. **Afonso PV, Ozden S, Prevost MC, Schmitt C, Seilhean D, Weksler B, Couraud PO, Gessain A, Romero IA, Ceccaldi PE.** 2007. Human blood-brain barrier disruption by retroviral-infected lymphocytes: role of myosin light chain kinase in endothelial tight-junction disorganization. J Immunol **179:**2576–2583. http://dx.doi.org/10.4049/jimmunol.179.4.2576.
13. **Troncoso MF, Ferragut F, Bacigalupo ML, Cardenas Delgado VM, Nugnes LG, Gentilini L, Laderach D, Wolfenstein-Todel C, Compagno D, Rabinovich GA, Elola MT.** 2014. Galectin-8: a matricellular lectin with key roles in angiogenesis. Glycobiology **24:**907–914. http://dx.doi.org/10.1093/glycob/cwu054.
14. **Weidle UH, Eggle D, Klostermann S, Swart GW.** 2010. ALCAM/CD166: cancer-related issues. Cancer Genomics Proteomics **7:**231–243.
15. **Poissonnier L, Villain G, Soncin F, Mattot V.** 2014. miR126-5p repression of ALCAM and SetD5 in endothelial cells regulates leucocyte adhesion and transmigration. Cardiovasc Res **102:**436–447. http://dx.doi.org/10.1093/cvr/cvu040.
16. **Swart GW, Lunter PC, Kilsdonk JW, Kempen LC.** 2005. Activated leukocyte cell adhesion molecule (ALCAM/CD166): signaling at the divide of melanoma cell clustering and cell migration? Cancer Metastasis Rev **24:**223–236. http://dx.doi.org/10.1007/s10555-005-1573-0.
17. **Cayrol R, Wosik K, Berard JL, Dodelet-Devillers A, Ifergan I, Kebir H, Haqqani AS, Kreymborg K, Krug S, Moumdjian R, Bouthillier A, Becher B, Arbour N, David S, Stanimirovic D, Prat A.** 2008. Activated leukocyte cell adhesion molecule promotes leukocyte trafficking into the central nervous system. Nat Immunol **9:**137–145. http://dx.doi.org/10.1038/ni1551.
18. **Yao H, Kim K, Duan M, Hayashi T, Guo M, Morgello S, Prat A, Wang J, Su TP, Buch S.** 2011. Cocaine hijacks sigma1 receptor to initiate induction of activated leukocyte cell adhesion molecule: implication for increased monocyte adhesion and migration in the CNS. J Neurosci **31:**5942–5955. http://dx.doi.org/10.1523/JNEUROSCI.5618-10.2011.
19. **Williams DW, Anastos K, Morgello S, Berman JW.** 2015. JAM-A and ALCAM are therapeutic targets to inhibit diapedesis across the BBB of

CD14+CD16+ monocytes in HIV-infected individuals. J Leukoc Biol **97:**401–412. http://dx.doi.org/10.1189/jlb.5A0714-347R.

20. **Williams DW, Calderon TM, Lopez L, Carvallo-Torres L, Gaskill PJ, Eugenin EA, Morgello S, Berman JW.** 2013. Mechanisms of HIV entry into the CNS: increased sensitivity of HIV infected CD14+CD16+ monocytes to CCL2 and key roles of CCR2, JAM-A, and ALCAM in diapedesis. PLoS One **8:**e69270. http://dx.doi.org/10.1371/journal.pone.0069270.
21. **Weksler BB, Subileau EA, Perriere N, Charneau P, Holloway K, Leveque M, Tricoire-Leignel H, Nicotra A, Bourdoulous S, Turowski P, Male DK, Roux F, Greenwood J, Romero IA, Couraud PO.** 2005. Blood-brain barrier-specific properties of a human adult brain endothelial cell line. FASEB J **19:**1872–1874.
22. **Cartier LM, Cea JG, Vergara C, Araya F, Born P.** 1997. Clinical and neuropathological study of six patients with spastic paraparesis associated with HTLV-I: an axomyelinic degeneration of the central nervous system. J Neuropathol Exp Neurol **56:**403–413. http://dx.doi.org/10.1097/00005072-199704000-00009.
23. **Albrecht D, Garcia L, Cartier L, Kettlun AM, Vergara C, Collados L, Valenzuela MA.** 2006. Trophic factors in cerebrospinal fluid and spinal cord of patients with tropical spastic paraparesis, HIV, and Creutzfeldt-Jakob disease. AIDS Res Hum Retroviruses **22:**248–254. http://dx.doi.org/10.1089/aid.2006.22.248.
24. **Chevalier SA, Durand S, Dasgupta A, Radonovich M, Cimarelli A, Brady JN, Mahieux R, Pise-Masison CA.** 2012. The transcription profile of Tax-3 is more similar to Tax-1 than Tax-2: insights into HTLV-3 potential leukemogenic properties. PLoS One **7:**e41003. http://dx.doi.org/10.1371/journal.pone.0041003.
25. **Pfaffl MW.** 2001. A new mathematical model for relative quantification in real-time RT-PCR. Nucleic Acids Res **29:**e45. http://dx.doi.org/10.1093/nar/29.9.e45.
26. **Sakaguchi S, Sakaguchi N, Asano M, Itoh M, Toda M.** 1995. Immunologic self-tolerance maintained by activated T cells expressing IL-2 receptor alpha-chains (CD25). Breakdown of a single mechanism of self-tolerance causes various autoimmune diseases. J Immunol **155:**1151–1164.
27. **Araya N, Sato T, Yagishita N, Ando H, Utsunomiya A, Jacobson S, Yamano Y.** 2011. Human T-lymphotropic virus type 1 (HTLV-1) and regulatory T cells in HTLV-1-associated neuroinflammatory disease. Viruses **3:**1532–1548. http://dx.doi.org/10.3390/v3091532.
28. **Villaudy J, Wencker M, Gadot N, Gillet NA, Scoazec JY, Gazzolo L, Manz MG, Bangham CR, Dodon MD.** 2011. HTLV-1 propels thymic human T cell development in "human immune system" Rag2(−)/(−) gamma c(−)/(−) mice. PLoS Pathog **7:**e1002231. http://dx.doi.org/10.1371/journal.ppat.1002231.
29. **Manivannan K, Rowan AG, Tanaka Y, Taylor GP, Bangham CR.** 2016. CADM1/TSLC1 identifies HTLV-1-infected cells and determines their susceptibility to CTL-mediated lysis. PLoS Pathog **12:**e1005560. http://dx.doi.org/10.1371/journal.ppat.1005560.
30. **Alais S, Mahieux R, Dutartre H.** 2015. Viral source-independent high susceptibility of dendritic cells to human T-cell leukemia virus type 1 infection compared to that of T lymphocytes. J Virol **89:**10580–10590. http://dx.doi.org/10.1128/JVI.01799-15.
31. **Higuchi M, Fujii M.** 2009. Distinct functions of HTLV-1 Tax1 from HTLV-2 Tax2 contribute key roles to viral pathogenesis. Retrovirology **6:**117. http://dx.doi.org/10.1186/1742-4690-6-117.
32. **Smith MR, Greene WC.** 1990. Identification of HTLV-I tax trans-activator mutants exhibiting novel transcriptional phenotypes. Genes Dev **4:**1875–1885. http://dx.doi.org/10.1101/gad.4.11.1875.
33. **Mori N, Yamada Y, Ikeda S, Yamasaki Y, Tsukasaki K, Tanaka Y, Tomonaga M, Yamamoto N, Fujii M.** 2002. Bay 11-7082 inhibits transcription factor NF-kappaB and induces apoptosis of HTLV-I-infected T-cell lines and primary adult T-cell leukemia cells. Blood **100:**1828–1834. http://dx.doi.org/10.1182/blood-2002-01-0151.
34. **King JA, Tan F, Mbeunkui F, Chambers Z, Cantrell S, Chen H, Alvarez D, Shevde LA, Ofori-Acquah SF.** 2010. Mechanisms of transcriptional regulation and prognostic significance of activated leukocyte cell adhesion molecule in cancer. Mol Cancer **9:**266. http://dx.doi.org/10.1186/1476-4598-9-266.
35. **Wang J, Gu Z, Ni P, Qiao Y, Chen C, Liu X, Lin J, Chen N, Fan Q.** 2011. NF-kappaB P50/P65 hetero-dimer mediates differential regulation of CD166/ALCAM expression via interaction with micoRNA-9 after serum deprivation, providing evidence for a novel negative auto-regulatory loop. Nucleic Acids Res **39:**6440–6455. http://dx.doi.org/10.1093/nar/gkr302.
36. **Sun SC, Yamaoka S.** 2005. Activation of NF-kappaB by HTLV-I and implications for cell transformation. Oncogene **24:**5952–5964. http://dx.doi.org/10.1038/sj.onc.1208969.
37. **Weksler B, Romero IA, Couraud PO.** 2013. The hCMEC/D3 cell line as a model of the human blood brain barrier. Fluids Barriers CNS **10:**16. http://dx.doi.org/10.1186/2045-8118-10-16.
38. **Nummer D, Suri-Payer E, Schmitz-Winnenthal H, Bonertz A, Galindo L, Antolovich D, Koch M, Buchler M, Weitz J, Schirrmacher V, Beckhove P.** 2007. Role of tumor endothelium in CD4+ CD25+ regulatory T cell infiltration of human pancreatic carcinoma. J Natl Cancer Inst **99:**1188–1199. http://dx.doi.org/10.1093/jnci/djm064.
39. **Walsh PT, Benoit BM, Wysocka M, Dalton NM, Turka LA, Rook AH.** 2006. A role for regulatory T cells in cutaneous T-cell lymphoma; induction of a CD4 + CD25 + Foxp3+ T-cell phenotype associated with HTLV-1 infection. J Invest Dermatol **126:**690–692. http://dx.doi.org/10.1038/sj.jid.5700121.
40. **Kress AK, Grassmann R, Fleckenstein B.** 2011. Cell surface markers in HTLV-1 pathogenesis. Viruses **3:**1439–1459. http://dx.doi.org/10.3390/v3081439.
41. **Bharadwaj AS, Schewitz-Bowers LP, Wei L, Lee RW, Smith JR.** 2013. Intercellular adhesion molecule 1 mediates migration of Th1 and Th17 cells across human retinal vascular endothelium. Invest Ophthalmol Vis Sci **54:**6917–6925. http://dx.doi.org/10.1167/iovs.13-12058.
42. **Reymond N, d'Agua BB, Ridley AJ.** 2013. Crossing the endothelial barrier during metastasis. Nat Rev Cancer **13:**858–870. http://dx.doi.org/10.1038/nrc3628.
43. **Te Riet J, Helenius J, Strohmeyer N, Cambi A, Figdor CG, Muller DJ.** 2014. Dynamic coupling of ALCAM to the actin cortex strengthens cell adhesion to CD6. J Cell Sci **127:**1595–1606. http://dx.doi.org/10.1242/jcs.141077.
44. **Tudor C, te Riet J, Eich C, Harkes R, Smisdom N, Bouhuijzen Wenger J, Ameloot M, Holt M, Kanger JS, Figdor CG, Cambi A, Subramaniam V.** 2014. Syntenin-1 and ezrin proteins link activated leukocyte cell adhesion molecule to the actin cytoskeleton. J Biol Chem **289:**13445–13460. http://dx.doi.org/10.1074/jbc.M113.546754.
45. **Ichinose K, Nakamura T, Kawakami A, Eguchi K, Nagasato K, Shibayama K, Tsujihata M, Nagataki S.** 1992. Increased adherence of T cells to human endothelial cells in patients with human T-cell lymphotropic virus type I-associated myelopathy. Arch Neurol **49:**74–76. http://dx.doi.org/10.1001/archneur.1992.00530250078019.
46. **Abadier M, Haghayegh Jahromi N, Cardoso Alves L, Boscacci R, Vestweber D, Barnum S, Deutsch U, Engelhardt B, Lyck R.** 2015. Cell surface levels of endothelial ICAM-1 influence the transcellular or paracellular T-cell diapedesis across the blood-brain barrier. Eur J Immunol **45:**1043–1058. http://dx.doi.org/10.1002/eji.201445125.
47. **Kim SJ, Nair AM, Fernandez S, Mathes L, Lairmore MD.** 2006. Enhancement of LFA-1-mediated T cell adhesion by human T lymphotropic virus type 1 p12I1. J Immunol **176:**5463–5470. http://dx.doi.org/10.4049/jimmunol.176.9.5463.